Sciencexpress Reports

# Electro-optical frequency division and stable microwave synthesis

**Jiang Li,[1]* Xu Yi,[1]* Hansuek Lee,[1] Scott A. Diddams,[2] Kerry J. Vahala[1]†**

[1]T. J. Watson Laboratory of Applied Physics, California Institute of Technology, Pasadena, CA 91125, USA.
[2]Time and Frequency Division, National Institute of Standards and Technology, Boulder, CO 80305, USA.

*These authors contributed equally to this work.

†Corresponding author. E-mail: vahala@caltech.edu

**Optical frequency division using frequency combs has revolutionized time keeping and the generation of stable microwave signals. We demonstrate optical frequency division and microwave generation by using a tunable electrical oscillator to create dual combs through phase modulation of two optical signals having a stable difference frequency. Phase-locked control of the electrical oscillator by optical frequency division produces stable microwaves. Our approach transposes the oscillator and frequency reference of a conventional microwave frequency synthesizer. In this way, the oscillator experiences large phase noise reduction relative to the frequency reference. The electro-optical approach additionally relaxes the need for highly-linear photodetection of the comb mode spacing. Besides simplicity, the technique is also tunable and scalable to higher division ratios.**

The photomixing of two, highly-coherent, laser signals is a well-known approach to generate a stable radio frequency or microwave signal (*1*, *2*). Recently, however, a different approach to all-optical, signal generation has been demonstrated that may revolutionize applications requiring high-stability microwaves. Rather than photomixing stabilized laser signals to directly produce a microwave signal, the approach uses an octave-spanning, self-referenced frequency comb to divide a stable optical reference frequency down to microwave or radio frequency rates (*3*). Frequency dividers are widely used in electronics to generate new frequencies from a single, base oscillator or to coherently link different frequency bands. As an ancillary benefit, all frequency dividers reduce the phase noise spectral density of the output signal relative to the input by the square of the division ratio. The new optical frequency dividers perform division by a factor of ~50,000 (the ratio of optical to microwave frequencies), so that phase-noise reduction is greater than $10^9$. Moreover, reference-cavity stabilized lasers exhibit a superior, fractional frequency stability in comparison to electrical oscillators (*4*, *5*). Optical dividers applied to such signals thereby generate microwave signals with an exceedingly-low phase noise level (*3*).

We present a way to generate high-performance microwave signals through optical frequency division (OFD) using a cascade of direct phase modulation and self-phase modulation to create an optical comb (*6–9*). Because the spectral line spacing is set by the electrical oscillator used to drive the phase modulators (as opposed to an optical resonator), the method of microwave synthesis has similarities to conventional microwave synthesizers while also leveraging the power of optical frequency division to reduce phase noise.

In our approach, two laser lines having good relative frequency stability provide an optical reference for the microwave source (Fig. 1A). These laser lines are produced by Brillouin oscillation in a single, high-Q microcavity. However, the lines could also result from any stable optical references, including various types of dual-mode lasers (*10–15*), two lasers locked to distinct optical modes of a reference cavity (*16*) or lasers stabilized to atomic transitions (*17*). The laser lines enter the frequency divider portion of the signal generator where they are phase modulated by a pair of modulators at a frequency set by a voltage-controlled, electrical oscillator (VCO). The sideband spectrum created by the phase modulators is further broadened by pulse forming and self phase modulation in an optical fiber (*8*, *18*, *19*). The comb of lines extending from each laser line results in a pair of sidebands near the mid point of the frequency span. These are optically filtered and detected. The detected beat note signal contains the phase noise of the VCO, but magnified by the optical division factor. It therefore provides a suitable error signal for phase-lock-loop control of the VCO.

It is interesting to contrast this microwave source based on electro-optical frequency division (EOFD) with a conventional microwave source based on electrical frequency division of a VCO (*20*). In the conventional approach (Fig. 1B), the VCO provides the highest frequency in the system. It is stabilized by electrical, frequency division and phase comparison to a lower-frequency, reference oscillator, such as a quartz oscillator. A consequence is that the stabilized VCO has a phase noise level that is always higher than the reference oscillator phase noise by the square of their frequency ratio (i.e., the frequency division ratio). In contrast, our optical version reverses the positions of the reference and the VCO in the frequency domain. Specifically, the reference is provided by the frequency difference of the laser lines and this frequency difference is made much greater than the frequency of the VCO (in the present implementation this is a non-detectable rate set at approximately 150 times the VCO frequency). Moreover, this reference frequency is divided down to the VCO frequency as opposed to dividing the VCO frequency down to the reference frequency rate. By making this reversal, the present device benefits from the stability of optical oscillators, and the power of optical frequency division to quadratically reduce the phase noise of optical oscillators by the division factor. Also, because the divider derives its rate from the electrical VCO, it is continuously tunable. In particular, the frequency output is set by the tuning range of the electrical VCO and the frequency separation of the reference laser lines and not fixed by a cavity repetition rate. Additionally, by obtaining the output of the electro-optical frequency divider directly from the VCO, this approach greatly relaxes the linearity constraints of high bandwidth photodetection that have posed significant challenges for OFD based on mode-locked lasers (*21*, *22*).

The use of a frequency difference as opposed to an absolute frequency to derive a reference for microwave generation has been demonstrated using mode-locked laser frequency combs. In that case the mode locked frequency comb optical divider is implemented by locking a comb at two frequencies of a reference cavity (*16*). This two-point lock approach has also been implemented using two atomic lines and a frequency microcomb (*17*). It is also interesting to note that cascaded phase modulation, besides being applied for pulse generation (*6–9*), has also been used to stabilize the frequency difference (in the millimeter wave domain) of a dual-frequency laser (*23*) and to create continuously tunable microwave signals by sideband-injection locking (*24*).

To understand phase noise reduction in this divider consider the accumulated phase noise contributions in the side bands as tracked from the laser sources to the phase difference of the detected sidebands (Fig.

1C). By adjusting the VCO phase to nullify the phase difference, $\Delta\phi$, the VCO fluctuations are reduced to: $\langle \phi_M^2 \rangle = \langle (\phi_1 - \phi_2)^2 \rangle / (N_1 + N_2)^2$, where $\phi_{1,2}$ and $\phi_M$ are the phase fluctuations of the laser field phases and the electrical VCO. Also, $N_1$ and $N_2$ are the number of sidebands produced by modulation (sidebands are higher in frequency for laser 1 and lower in frequency for laser 2). As a result, within the servo control bandwidth, the phase noise of the VCO is given by the relative phase noise of the two laser fields reduced by the division factor squared $(N_1 + N_2)^2$. Clearly, to reduce phase noise of the electrical VCO, the laser frequency separation should be made as large as possible. In the present system, this value is set by the span of the dual-pumped Brillouin lasers. It is also important to note that it is the relative-phase-noise of the laser sources that determines the phase noise reference level (before optical frequency division). Because these lasers are co-lasing within the same resonator the common-mode laser noise (e.g., pump noise, microphonics, cavity noise) is largely suppressed, leaving primarily fundamental sources of laser noise such as Schawlow-Townes noise.

In the experimental setup (Fig. 2), the reference laser signals are provided by Brillouin-laser lines co-lasing within a single silica-on-silicon high-Q disk resonator. The coherence properties of the individual Brillouin laser lines is excellent (*25*, *26*). The silica disk resonators are designed and fabricated with a free-spectral-range (FSR) of 10.890 GHz that matches the Brillouin shift frequency in silica near 1550 nm. A frequency modulation technique is used to measure the FSR (*27*). In prior work a single pump configuration was used to demonstrate microwave synthesis up to K-band (22 GHz) rates by photomixing of cascaded Brillouin laser lines (*28*). Here the Brillouin lines must be separated by a much larger frequency and a dual pump configuration is used. Each pump laser is locked to the disk resonator using the Pound-Drever-Hall (PDH) technique (*29*) and excites its own Brillouin laser in the backward-propagating direction. In the experiment, the SBS lines are separated by as much as 1.61 THz by dual pumping on cavity modes separated by 148 FSR using the independently tunable CW lasers. The maximum separation of 1.61 THz is currently set by the tuning range of the pump lasers. The optical spectra of the dual SBS lines at several frequency differences appears in Fig. 3A. Besides inherent stability from co-lasing within the same cavity, it is worth noting that the two SBS laser signals share the same fiber optical path, thereby suppressing path length variation effects.

The laser signals are coupled to the optical divider section using a circulator. In order to increase the comb bandwidth and thereby also the division factor, two phase modulators with low $V_\pi \sim 3.9$V (at 12 GHz) are cascaded and phase synchronized with a RF phase shifter. The phase modulators were driven at 32.5 dBm and 30.7 dBm, corresponding to a total phase modulation amplitude up to $6\pi$ ($\approx \pi[(V_{drive})/(V_\pi)]$), which is also approximately equal to half of the number of sidebands produced by the modulators (*30*). In the experiment, up to 30 EOM sidebands can be created using the phase modulators alone, enabling optical division by around a factor of 30. An optical spectrum showing both the original SBS laser lines (18 FSR frequency separation) and the resulting phase modulation sidebands is shown in Fig. 3B. To further enhance the sideband spectral width, pulse broadening is performed by introducing an intensity modulator, dispersion compensation, erbium-doped fiber amplifier (EDFA), and nonlinear fiber (*8*, *18*, *19*). The inner sidebands are optically filtered and their beat note is detected on an amplified photodetector. The beat note frequency was set near 10 MHz and phase compared with a 10 MHz oven-controlled crystal oscillator (OCXO) to generate the error signal used for phase locking the VCO. The phase noise of the OCXO is very low (compared with the optical frequency reference) and is further divided down in the control loop (supplementary materials). As such, it does not introduce any limitation on the final VCO phase noise. The residual phase noise levels of the amplifier used here [MicroSemi model L0612-35-T977] are well below the phase noise levels attained by loop control of the VCO and therefore do not present any limitation to the measurement. It is also important to note that the sum of the free-running VCO phase noise and the residual phase noise of the RF power amplifier is suppressed by the servo loop (see Supplementary Materials). As a result, by taking the electrical output signal at the output of the amplifier there is no phase noise limitation set by the RF power amplifier.

The phase noise reference level is set by the relative phase noise of the co-lasing Brillouin laser lines. This phase noise level is expected to be relatively insensitive to the frequency difference (*26*, *28*). Therefore, this noise level was measured by pumping the two lasers on modes that were three cavity FSR apart, enabling direct detection of the beat signal at 32.7 GHz by a fast photodetector. This detected signal is then analyzed using a phase noise analyzer to obtain the single sideband (SSB) phase noise spectrum (Fig. 3C, red curve). For offset frequencies higher than 100 Hz this spectrum is limited by Schawlow-Townes noise while at offset frequencies less than 100 Hz a technical noise component is present (*28*). The white phase noise floor above 1 MHz offset is due to the thermal noise of the fast photodetector. The SSB phase noise spectrum is measured using a commercial phase noise tester (Rohde Schwartz model FSUP26—sensitivity limit given as the cyan square markers in Fig. 3C) which is based on the phase detector method with dual-channel cross-correlations to further improve the phase noise sensitivity.

To test the optical divider, the VCO is locked to the divided optical reference using the VCO control/tuning port (Fig. 2). The blue and green curves in Fig. 3C are the corresponding phase noise spectra of the VCO at 10.89 GHz when optically dividing by 30 and 148 times relative to the initial frequency separation of the dual SBS lines at 327 GHz and 1.61 THz, respectively. The microwave carrier frequency is held at 10.89 GHz in these measurements by adjusting the frequency separation of the Brillouin laser lines using the tunable pump lasers. Decrease of the phase noise with the increase of the division ratio is clear in the data. For division by 148x, the achieved phase noise level is –104 dBc/Hz at 1 kHz and –121 dBc/Hz at 10 kHz. For comparison, the dashed, black curve in Fig. 3C gives the phase noise of the free running VCO. The servo locking bandwidth can be seen from the servo bumps in the phase noise spectra, which are located at 820 kHz for the blue curve (adopting path I in Fig. 2) and 300 kHz for the green curve (adopting path II in Fig. 2). As an aside, the locking bandwidth is determined by the loop delay, which includes both optical and electrical path lengths (~20 m for path I and ~50 m for path II), and the FM response of the VCO. For frequencies beyond the servo control bandwidth, the phase noise level is set by the free-running VCO.

In the measured RF power spectra of the VCO at 10.89 GHz (20 kHz span and 30 Hz resolution bandwidth) (Fig. 3D), the black curve is the free running VCO spectrum, while the red, blue and green curves are the spectra of the phase locked VCO when dividing down 18, 30 and 148 times from corresponding SBS frequency separations of 196 GHz, 327 GHz and 1.61 THz. Figure 3E summarizes these results by giving the measured phase noise at 1 kHz, 10 kHz and 100 kHz offset frequencies plotted versus division ratios of 1, 3, 4, 10, 18, 30 and 148. The dashed lines give $1/N^2$ trend lines. For comparison, the phase noise of an Agilent MXG microwave synthesizer [carrier 11 GHz, offset 100 kHz, Agilent online data sheet, Literature number 5989-7572EN] and a high performance Agilent PSG microwave synthesizer [carrier 11 GHz, offset 100 kHz, Agilent online data Sheet, Literature number 5989-0698EN, option UNX] are shown as black, dashed and dotted lines.

So far, the microwave frequency has been fixed, however, this can be adjusted by varying the division ratio, $N$, and the VCO frequency for a fixed separation of the dual SBS lines $\nu_1 - \nu_2$ as in Fig. 4A (i.e., $f_M = [(\nu_1 - \nu_2 \pm \delta f)/(N)]$). Figure 4B shows the RF spectrum of a phase locked 12.566 GHz carrier with a division factor of 26, while Fig. 4C shows the

RF power spectrum of a microwave signal at 9.075 GHz with a divison factor of 36 (in both cases, the dual SBS frequency difference is set at 327 GHz). Moreover, the initial reference frequency difference can also be tuned so that a wide range of final microwave frequencies can be derived from a single divider.

The optical division factor can be scaled to higher values for additional phase noise improvement. While the frequency reference might be based on some other system, for simplicity we consider using one SBS laser operating at 1.55 microns (current system) and another at 1 micron [recently demonstrated using silica high-Q disks (*31*)]. Matching the Brillouin shift at these wavelengths within the same disk is possible by designing the system to oscillate at a multiple cavity free spectral range. For example, a disk diameter of ~ 12 mm (FSR ~5.4 GHz, which is half of the Brillouin shift at 1.55 micron and one third of the Brillouin shift at 1 micron.) would enable simultaneous SBS oscillation at 1.55 micron and 1 micron. To extend the comb over this span would require about one half of an octave. Spectrally-broadened EOM combs with more than 500 nm bandwidth have previously been demonstrated (*32*). An electro-optical frequency divider spanning 1 micron and 1.55 micron SBS lines is therefore feasible. This example system does not necessarily represent a fundamental limit, but nonetheless would feature a division factor of approximately 7000. Assuming that relative phase noise of the co-lasing optical lines does not degrade beyond what has been demonstrated in the present work, this hypothetical system could provide phase noise performance close to levels demonstrated by conventional OFD.

This new photonic architecture for optical frequency division provides a route to improve the phase noise of a common VCO. In the present configuration, dual SBS lasers have been co-generated in a single, chip-based resonator to establish a stable reference as high as 1.61 THz. While dual pumped SBS laser lines provide an excellent reference frequency, it should also be possible to lock two lasers to a resonator to establish the reference. As the current frequency separation is limited by the pump lasers, much larger division ratios and potentially lower phase noise levels should be possible. In comparison to conventional optical frequency division using a self-referenced frequency comb, this technique does not presently offer as large a division ratio. However, it is simple, relatively low cost and also provides tuning of the electrical carrier. Moreoever, it relies upon a reference signal derived from the relative phase of two lasers as opposed to the absolute phase of a single laser. This can potentially improve the robustness with respect to microphonics and other sources of technical noise.

**References and Notes**


1. A. J. Seeds, K. J. Williams, Microwave Photonics. *J. Lightwave Technol.* **24**, 4628–4641 (2006). doi:10.1109/JLT.2006.885787
2. J. Yao, Microwave Photonics. *J. Lightwave Technol.* **27**, 314–335 (2009). doi:10.1109/JLT.2008.2009551
3. T. Fortier, M. S. Kirchner, F. Quinlan, J. Taylor, J. C. Bergquist, T. Rosenband, N. Lemke, A. Ludlow, Y. Jiang, C. W. Oates, S. A. Diddams, Generation of ultrastable microwaves via optical frequency division. *Nat. Photonics* **5**, 425–429 (2011). doi:10.1038/nphoton.2011.121
4. B. Young, F. Cruz, W. Itano, J. Bergquist, Visible Lasers with Subhertz Linewidths. *Phys. Rev. Lett.* **82**, 3799–3802 (1999). doi:10.1103/PhysRevLett.82.3799
5. T. Kessler, C. Hagemann, C. Grebing, T. Legero, U. Sterr, F. Riehle, M. J. Martin, L. Chen, J. Ye, A sub-40-mHz-linewidth laser based on a silicon single-crystal optical cavity. *Nat. Photonics* **6**, 687–692 (2012). doi:10.1038/nphoton.2012.217
6. H. Murata, A. Morimoto, T. Kobayashi, S. Yamamoto, Optical pulse generation by electrooptic-modulation method and its application to integrated ultrashort pulse generators. *IEEE J. Sel. Top. Quantum Electron.* **6**, 1325–1331 (2000). doi:10.1109/2944.902186
7. M. Fujiwara, J. Kani, H. Suzuki, K. Araya, M. Teshima, Flattened optical multicarrier generation of 12.5 GHz spaced 256 channels based on sinusoidal amplitude and phase hybrid modulation. *Electron. Lett.* **37**, 967–968 (2001). doi:10.1049/el:20010612
8. C. B. Huang, S. G. Park, D. E. Leaird, A. M. Weiner, Nonlinearly broadened phase-modulated continuous-wave laser frequency combs characterized using DPSK decoding. *Opt. Express* **16**, 2520–2527 (2008). Medline doi:10.1364/OE.16.002520
9. A. J. Metcalf, V. Torres-Company, D. E. Leaird, A. M. Weiner, High-Power Broadly Tunable Electrooptic Frequency Comb Generator. *IEEE J. Sel. Top. Quantum Electron.* **19**, 3500306 (2013). doi:10.1109/JSTQE.2013.2268384
10. G. Pillet, L. Ï. Morvan, M. Brunel, F. Bretenaker, D. Dolfi, M. Vallet, J.-P. Huignard, A. Le Floch, Dual-Frequency Laser at 1.5 $$ m for Optical Distribution and Generation of High-Purity Microwave Signals. *J. Lightwave Technol.* **26**, 2764–2773 (2008). doi:10.1109/JLT.2008.927209
11. J. Geng, S. Staines, S. Jiang, Dual-frequency Brillouin fiber laser for optical generation of tunable low-noise radio frequency/microwave frequency. *Opt. Lett.* **33**, 16–18 (2008). Medline doi:10.1364/OL.33.000016
12. S. Pan, J. Yao, A wavelength-switchable single-longitudinal-mode dual-wavelength erbium-doped fiber laser for switchable microwave generation. *Opt. Express* **17**, 5414–5419 (2009). Medline doi:10.1364/OE.17.005414
13. M. C. Gross, P. T. Callahan, T. R. Clark, D. Novak, R. B. Waterhouse, M. L. Dennis, Tunable millimeter-wave frequency synthesis up to 100 GHz by dual-wavelength Brillouin fiber laser. *Opt. Express* **18**, 13321–13330 (2010). Medline doi:10.1364/OE.18.013321
14. P. T. Callahan, M. C. Gross, M. L. Dennis, Frequency-Independent Phase Noise in a Dual-Wavelength Brillouin Fiber Laser. *IEEE J. Quantum Electron.* **47**, 1142–1150 (2011). doi:10.1109/JQE.2011.2160047
15. G. Carpintero, E. Rouvalis, K. Ławniczuk, M. Fice, C. C. Renaud, X. J. Leijtens, E. A. Bente, M. Chitoui, F. Van Dijk, A. J. Seeds, 95 GHz millimeter wave signal generation using an arrayed waveguide grating dual wavelength semiconductor laser. *Opt. Lett.* **37**, 3657–3659 (2012). Medline doi:10.1364/OL.37.003657
16. W. C. Swann, E. Baumann, F. R. Giorgetta, N. R. Newbury, Microwave generation with low residual phase noise from a femtosecond fiber laser with an intracavity electro-optic modulator. *Opt. Express* **19**, 24387–24395 (2011). Medline doi:10.1364/OE.19.024387
17. S. B. Papp *et al*., arXiv:1309.3525 (2013).
18. I. Morohashi, T. Sakamoto, H. Sotobayashi, T. Kawanishi, I. Hosako, Broadband wavelength-tunable ultrashort pulse source using a Mach-Zehnder modulator and dispersion-flattened dispersion-decreasing fiber. *Opt. Lett.* **34**, 2297–2299 (2009). Medline doi:10.1364/OL.34.002297
19. A. Ishizawa, T. Nishikawa, A. Mizutori, H. Takara, A. Takada, T. Sogawa, M. Koga, Phase-noise characteristics of a 25-GHz-spaced optical frequency comb based on a phase- and intensity-modulated laser. *Opt. Express* **21**, 29186–29194 (2013). Medline doi:10.1364/OE.21.029186
20. U. L. Rohde, Microwave and wireless synthesizers: theory and design (Wiley, New York, 1997).
21. E. N. Ivanov, S. A. Diddams, L. Hollberg, Study of the excess noise associated with demodulation of ultra-short infrared pulses. *IEEE Trans. Ultrason. Ferroelectr. Freq. Control* **52**, 1068–1074 (2005). Medline doi:10.1109/TUFFC.2005.1503992
22. J. Taylor, S. Datta, A. Hati, C. Nelson, F. Quinlan, A. Joshi, S. Diddams, Characterization of Power-to-Phase Conversion in High-Speed P-I-N Photodiodes. *IEEE Photon. J.* **3**, 140–151 (2011). doi:10.1109/JPHOT.2011.2109703
23. A. Rolland, G. Loas, M. Brunel, L. Frein, M. Vallet, M. Alouini, Non-linear optoelectronic phase-locked loop for stabilization of opto-millimeter waves: Towards a narrow linewidth tunable THz source. *Opt. Express* **19**, 17944–17950 (2011). Medline doi:10.1364/OE.19.017944
24. G. J. Schneider, J. A. Murakowski, C. A. Schuetz, S. Shi, D. W. Prather, Radiofrequency signal-generation system with over seven octaves of continuous tuning. *Nat. Photonics* **7**, 118–122 (2013). doi:10.1038/nphoton.2012.339
25. H. Lee, T. Chen, J. Li, K. Y. Yang, S. Jeon, O. Painter, K. J. Vahala, Chemically etched ultrahigh-Q wedge-resonator on a silicon chip. *Nat. Photonics* **6**, 369–373 (2012). doi:10.1038/nphoton.2012.109
26. J. Li, H. Lee, T. Chen, K. J. Vahala, Characterization of a high coherence, Brillouin microcavity laser on silicon. *Opt. Express* **20**, 20170–20180 (2012). Medline doi:10.1364/OE.20.020170
27. J. Li, H. Lee, K. Y. Yang, K. J. Vahala, Sideband spectroscopy and dispersion measurement in microcavities. *Opt. Exp.* **20**, 26337–26344 (2012).

doi:10.1364/OE.20.026337
28. J. Li, H. Lee, K. J. Vahala, Microwave synthesizer using an on-chip Brillouin oscillator. *Nat. Commun.* **4**, 2097 (2013). Medline
29. R. Drever, J. L. Hall, F. Kowalski, J. Hough, G. Ford, A. Munley, H. Ward, Laser phase and frequency stabilization using an optical resonator. *Appl. Phys. B* **31**, 97–105 (1983). doi:10.1007/BF00702605
30. T. Sakamoto, T. Kawanishi, M. Izutsu, Asymptotic formalism for ultraflat optical frequency comb generation using a Mach-Zehnder modulator. *Opt. Lett.* **32**, 1515–1517 (2007). Medline doi:10.1364/OL.32.001515
31. J. Li, H. Lee, K. J. Vahala, Low-noise Brillouin laser on a chip at 1064 nm. *Opt. Lett.* **39**, 287–290 (2014). Medline doi:10.1364/OL.39.000287
32. S. Suzuki *et al*., paper NM3A.3, Nonlinear Optics Conference (NLO 2013), Optical Society of America.
33. F. M. Gardner, Phaselock Techniques, 3rd Ed. (Wiley, New York, 2005).
**Acknowledgments:** This work was sponsored by the DARPA ORCHID and PULSE programs and the Caltech IQIM. The authors also acknowledge support from the Kavli NanoScience Institute at Caltech. S.A.D acknowledges the support from Gordon and Betty Moore Foundation as a Moore Scholar at Caltech.

**Supplementary Materials**
www.sciencemag.org/content/science.1252909/DC1
Materials and Methods
Supplementary Text
Fig. S1
References (*33*)

4 March 2014; accepted 5 June 2014
Published online 19 June 2014
10.1126/science.1252909

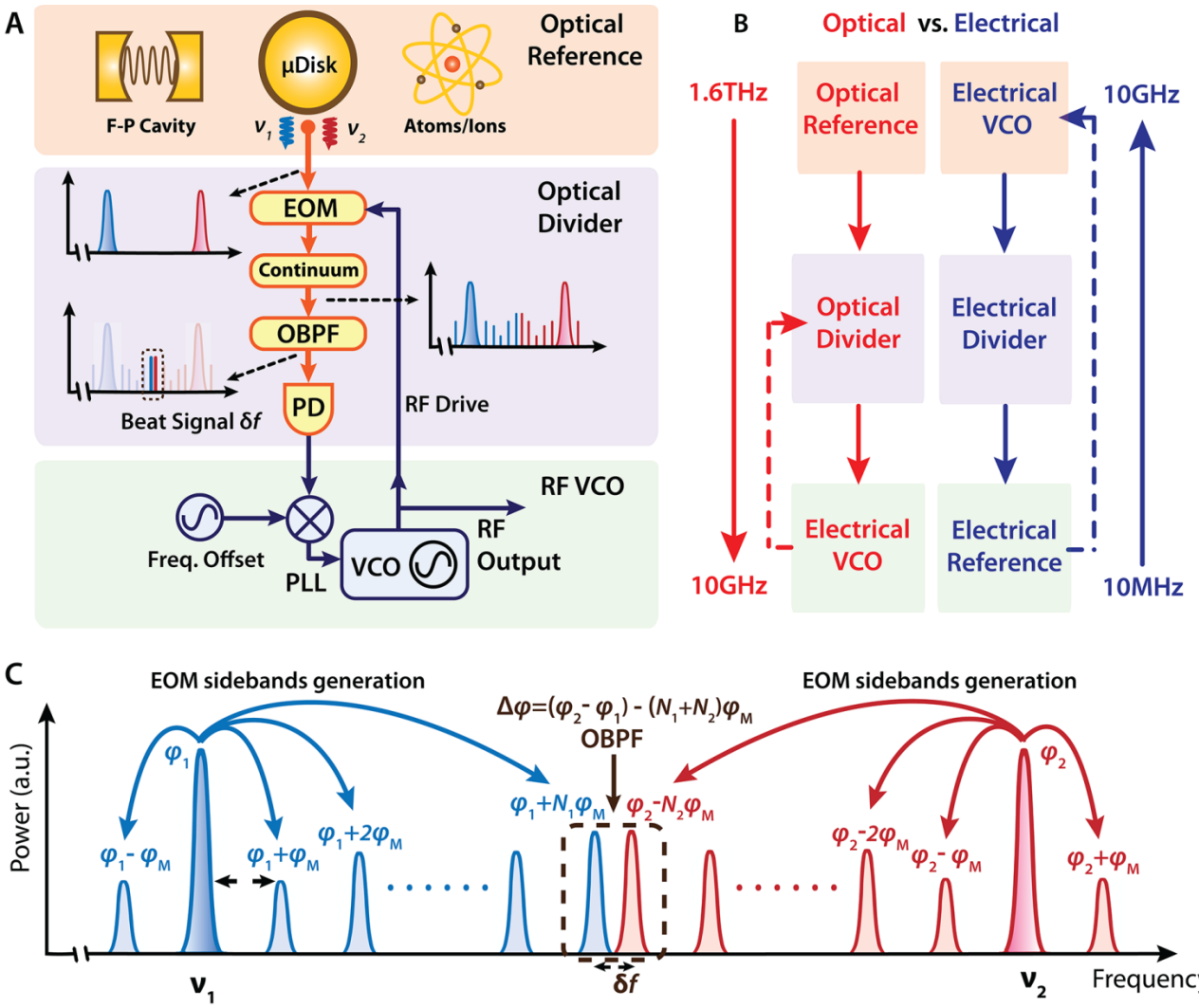


**Fig. 1. Conceptual schematics of stable microwave synthesis using cascaded phase modulation.** (**A**) Two, optical reference laser lines are provided by one of several possible methods, including dual-mode laser action (as described here), frequency locking two lasers to distinct optical modes of a reference cavity, or lasers stabilized to atomic transitions. These laser lines are phase modulated to produce sidebands, two of which nearly overlap at the spectral midpoint of the laser lines. The drive frequency is provided by the electrical VCO that is to be stabilized. Optical filtering and detection of the nearly overlapping sidebands gives a beatnote that is used to phase lock the VCO and lower its phase noise. EOM is electro-optical modulator, OBPF is optical band-pass filter, and PD is photodetector. (**B**) Comparison of conventional, electrical, phase-locked-loop control of a VCO with the present method is shown. The conventional method divides the VCO for phase comparison with the low frequency reference while the present method divides the frequency separation of two lasers to stabilize the electrical VCO. (C) Analysis of the relative phase of the inner side bands in the optical spectrum. $\phi_{1,2}$ and $\phi_M$ are the phase fluctuations of the laser field phases and the electrical VCO.

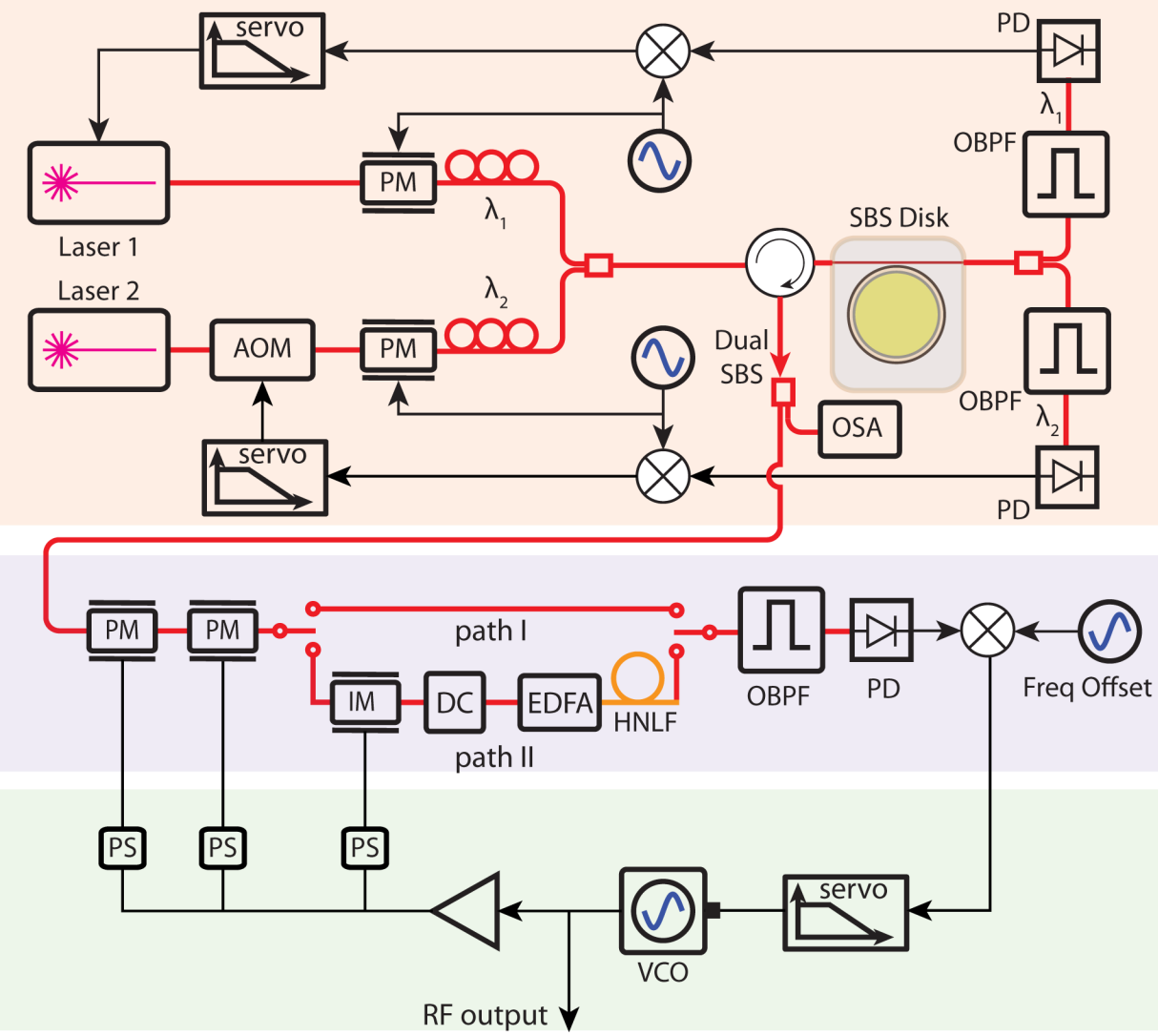


**Fig. 2. Experimental setup.** The upper block of the schematic shows the arrangement used for dual pumping of the disk-resonator Brillouin laser. Laser 1 and laser 2 are locked to distinct modes of a high Q disk resonator. Servo control involves direct frequency tuning of laser 1 and frequency shifting via an acousto-optic modulator (AOM) for laser 2. The reference laser lines provided by the Brillouin oscillation are input to the optical division function. Depending upon the desired division ratio two pathways are taken (Path I and Path II). For division up to 30x, a pair of phase modulators are synchronously driven, while for larger division ratios the phase modulators are cascaded with a fiber pulse broadener containing an intensity modulator (IM), dispersion compensation (DC), EDFA, and nonlinear fiber (HNLF). The filtered (OBPF) and detected signal is then processed for servo control of the VCO. Also shown are optical spectrum analyzer (OSA) and electrical phase shifters (PS).

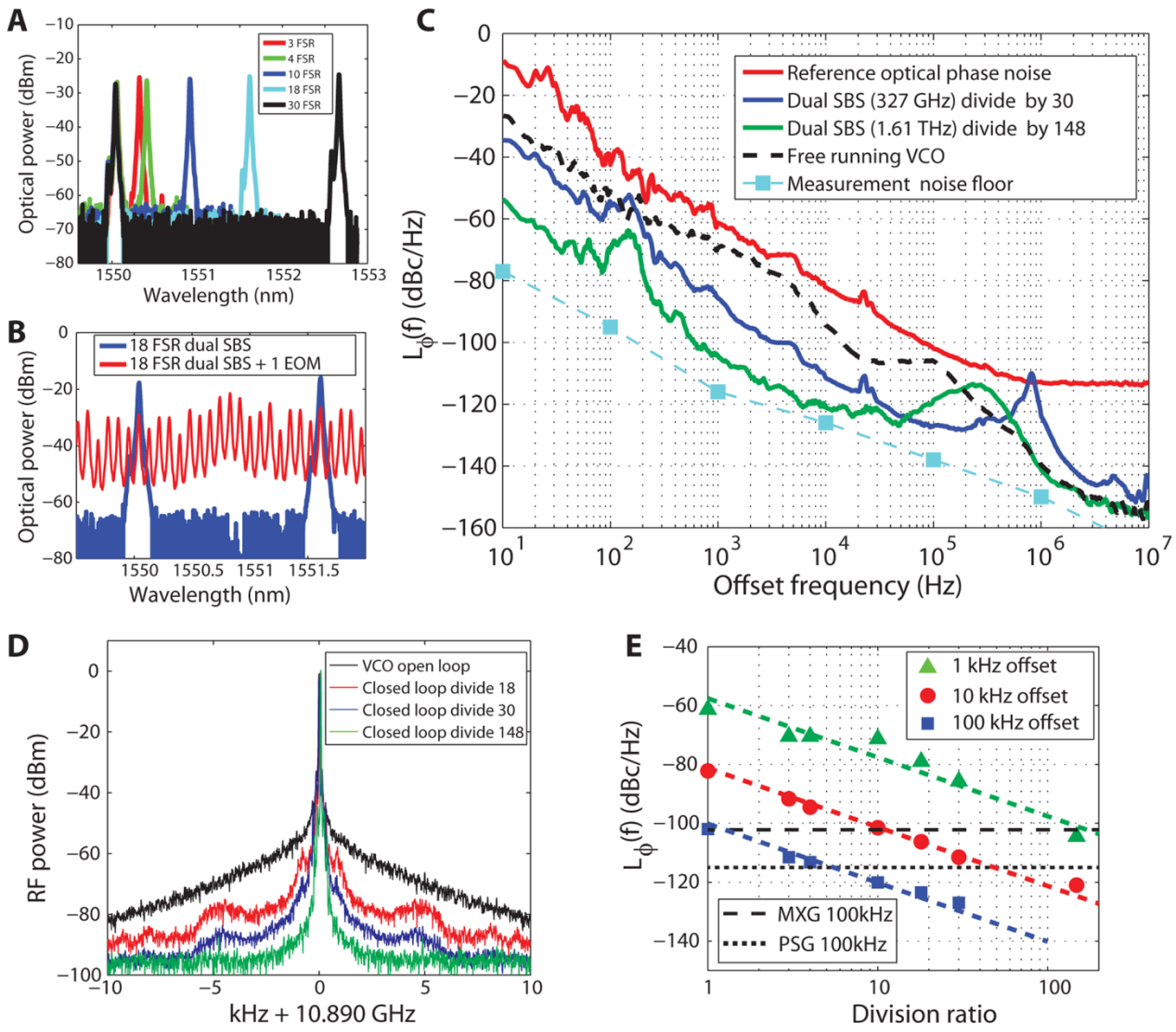


**Fig. 3. Summary of experimental data.** (**A**) Optical spectra of co-lasing Brillouin lasers at various tuning configurations used in the measurement corresponding to cavity FSR spacings provided in the inset. (**B**) Optical spectrum of Brillouin laser lines with (red) and without (blue) phase modulation. (**C**) Single sideband (SSB) phase noise spectra of the optical reference (red) is shown. For this measurement the dual SBS lines are tuned to a detectable frequency difference. Also shown are the closed-loop VCO phase noise referenced to dual SBS lines separated by 327 GHz (blue) and 1.61 THz (green) with corresponding division ratios of 30 and 148. The dashed, black curve is the phase noise of the free-running VCO. The cyan square markers denote the phase noise sensitivity of the phase noise tester. (**D**) VCO radio frequency power spectrum at 10.89 GHz for open loop and closed loop conditions in which the Brillouin frequency separation is divided by 18x, 30x, and 148x. Resolution bandwidth is set at 30 Hz. (**E**) Summary of SSB phase noise levels at 10.89 GHz versus optical division ratio. Cases shown are measured at 1, 10 and 100 kHz offset frequencies. The dashed lines give $1/N^2$ trends. Phase noise levels for an Agilent MXG and PSG microwave sources (carrier 11 GHz, 100 kHz offset) are provided for comparison.

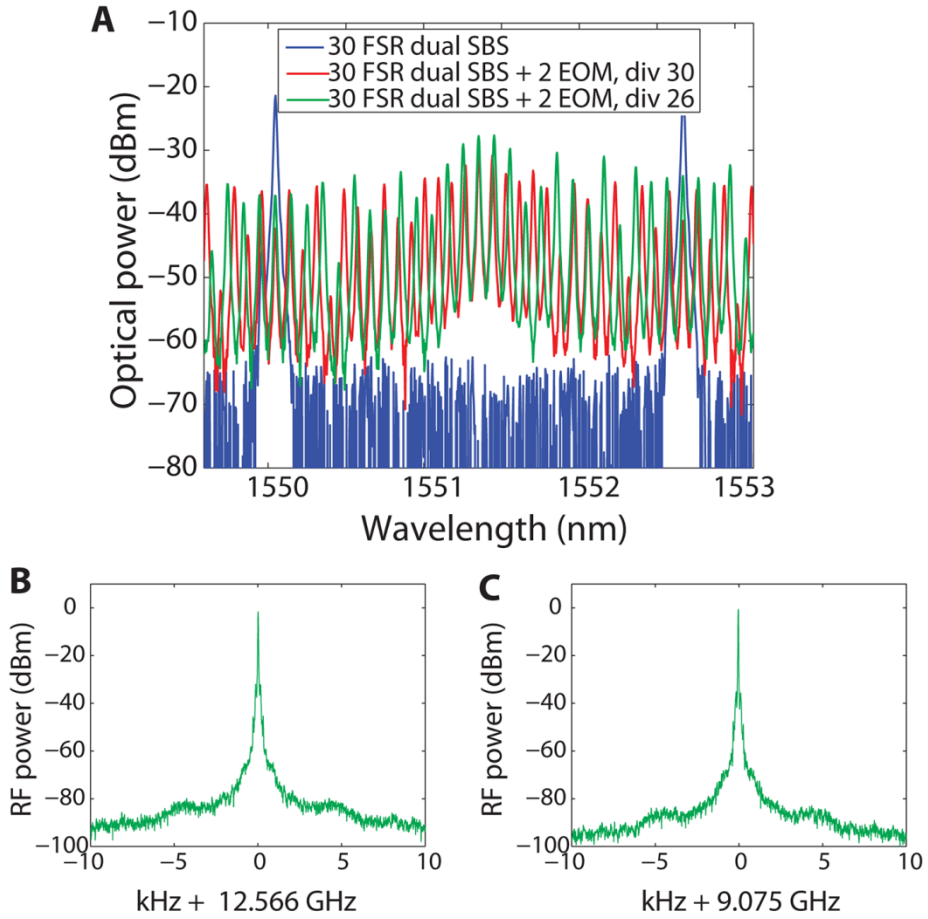


**Fig. 4. Demonstration of tuning of the phase-locked VCO frequency.** (**A**) Optical spectrum showing two Brillouin reference laser lines (blue) and tuning of the optical division by variation of the VCO modulation frequency to produce two different combs. (**B**) Radio frequency power spectrum corresponding to division by 26x to produce a 12.566 GHz electrical carrier frequency (resolution bandwidth is 30 Hz). (**C**) Radio frequency power spectrum corresponding to division by 36x to produce a 9.075 GHz electrical carrier frequency (resolution bandwidth is 30 Hz).